JOTCS A
Journal of the Turkish Chemical Society
Section: A
Chemistry
TURKISH CHEMICAL SOCIETY

A facile green synthesis of LDH nanosheets using sugar molecules

Ahmad Faiz Abdul Latip*[1], Mineesha Sivakumar[1], Faiz Bukhari Mohd Suah[1], Mohd Hazwan Hussin[1] and Mohd Zobir Hussein[2]

[1]School of Chemical Sciences, Universiti Sains Malaysia, Penang, Malaysia
[2]Institute of Advanced Technology, Universiti Putra Malaysia, Selangor, Malaysia

Abstract: The exfoliation of LDH materials is highly favorable for the formation of single-layer layered double hydroxides (LDH) nanosheets due to their unique chemical, thermal, optics, and biological properties. The green method for the exfoliation of layered double hydroxides (LDH) offers several advantages compared to conventional methods because it is considered safe, cost-effective, and eco-friendly. This report focuses on the exfoliation of layered double hydroxides (LDH) using sugar molecules as a green exfoliating agent without having to first pre-intercalate the layered material. The exfoliation of LDH is confirmed by X-ray diffraction (XRD), Fourier transform infrared spectroscopy (FTIR), transmission electron microscopy (TEM), thermogravimetric (TGA), differential scanning calorimetry (DSC), and Brunauer-Emmett-Teller (BET) analyses. We also examined the crystalline phase of LDH in different stages of liquid exfoliation; suspension, semi-dry suspension, and dried solid samples using XRD. XRD data shows one broad peak for all the LDH exfoliated samples at 2θ = 23.9°,22.4°, and 22.3° respectively, which correspond to the characteristic (006) basal reflection of LDH single layers. These single peaks indicate the formation of LDH nanosheets. The higher intensity peak at the region 1000-1020 cm^{-1} for LDH exfoliated samples indicates the successful exfoliation of sugar molecules in the interlayer of LDH. In BET, the wide hysteresis loop for the exfoliated LDHs proved the successful exfoliation of sugar molecules into LDH layers. TEM images show ultrathin sheets of LDH and spherical-like particles. This work shows that LDH nanosheets can be obtained by using green biomolecules through simple synthetic methods.

Keywords: Green synthesis, layered double hydroxide (LDH), exfoliation, sugar molecules, LDH nanosheets.

Submitted: March 26, 2024. **Accepted:** May 19, 2024.

Cite this: Abdul Latip AF, Sivakumar M, Mohd Suah FB, Hussin MH, Hussein MZ. A facile green synthesis of LDH nanosheets using sugar molecules. JOTCSA. 2024;11(3):967–80.

DOI: https://doi.org/10.18596/jotcsa.1458997.

***Corresponding author. E-mail:** afaiz@usm.my.

1. INTRODUCTION

Layered double hydroxide (LDH) is a two-dimensional (2D) layered material that belongs to the hydrotalcite-like (HT) compound group. LDH is represented by the formula $[M_{1-x}^{2+} M_x^{3+} (OH)_2]^{x+}\cdot[A_{x/n}]^{n-}\cdot mH_2O$, where M^{2+} and M^{3+} are divalent and trivalent cations and An- are inorganic or organic anions (1). The exchangeable interlayer anions, A^{n-} in the layered structure render the compounds such a unique material for intercalation chemistry (2). When these layers are exfoliated, nanosheets of LDH can be obtained, which are typically in the nanometer range (3). Over the past few decades, research into the exfoliation chemistry of LDH has seen a sharp increase (3). The exfoliation of LDH is the process of breaking apart the LDH multilayers into single layers consisting of nanosheets (4, 5). The LDH nanosheets display unique mechanical, optical, and biological properties compared to their bulky counterparts. Interestingly, liquid-phase exfoliation is one of the promising routes for exfoliating layered materials (3). This top-down approach has several advantages since they are easy to operate, versatile, and easily scalable (3). Several reports have dealt with the exfoliation of LDH in different solvents. However, using organic solvents as exfoliating solvents can be harmful as it is likely to harm the health of humans, animals, and plants (6). Adachi-Pagano et al.(2000) reported the exfoliation of ZnAl-LDH in organic solvent using

dodecyl sulfate (DDS) and butanol (7). Hibino and Jones et al.(2001) employed glycinate-containing MgAl-LDH in formamide at room temperature (5). Jobbagy and Regazzoni et al.(2004) studied the exfoliation of Mg-Al-DDS in toluene and CCl_4 (8). Previously researchers used organic solvents which are more toxic therefore, it is essential to use less toxic and more sustainable solvents to minimize the impact on the environment and human health. In this work, we demonstrate the green synthesis of LDH nanosheets using sugar molecules to exfoliate LDH without having to first pre-intercalate the layered material in dimethyl sulphoxide (DMSO). DMSO is a highly potential solvent for exfoliation due to its higher dielectric constant and low toxicity profile. DMSO is also miscible with water and most organic liquids (9). Sugar molecules are readily available, renewable, and non-toxic carbohydrates (10). It contains a large number of hydroxyl groups which may greatly facilitate the exfoliation of layered materials (11). When sugar molecules are intercalated between LDH layers, the functional groups of the sugars may influence the hydrogen bonds between the hydroxyl groups of intercalated molecules and the hydroxyl groups of basal layers of LDH. This may further lead to breaking the layers apart (11). It has been previously reported that sugar crystals are used to exfoliate boron nitride lamellae in water due to covalent interactions (12). Chen and co-workers investigated the interactions of natural sugars with inorganic layered nanomaterials, using natural sugar as a green exfoliating agent to exfoliate transition-metal dichalcogenides (TMDs) (11). Furthermore, the reports on structural studies have been reported by Joensen et al. on XRD study on single-layer and restacked MoS_2 (13). The structural studies of a single layer of MoS_2 in aqueous suspension show that a single layer differs from a bulk single crystal. When single-layer MoS_2 suspension dries up, a new phase is obtained, whereas in dry restacked MoS_2, bulk Mo-Mo distance starts to reappear. Sasaki et al. reported a stable colloidal suspension of an exfoliated titanate and the ensuing reassembling process (14). The layered protonic titanate was successfully exfoliated into single-layer nanosheets and the delaminated nanosheets were restacked upon drying; this reassembling process revealed the macromolecule aspects for the obtained individual nanosheets. XRD data showed that the amorphous halo changed into well well-order crystalline pattern upon drying. However, to our best knowledge, only limited studies have been reported on the structural information of the layered material in different sample phases using the X-ray diffraction (XRD) technique. This study demonstrates for the first time the crystalline phase of LDH in different stages of liquid exfoliation; suspension, semi-dry suspension, and dried solid samples.

2. EXPERIMENTAL SECTION

2.1. Reagents

Magnesium nitrate hexahydrate [$Mg(NO_3)_2.6H_2O$] and aluminium nitrate nanohydrate [$Al(NO_3)_3.9H_2O$] were purchased from Sigma-Aldrich. Sodium hydroxide (NaOH) and dimethyl sulfoxide (DMSO) were purchased from Merck. Sucrose, glucose, and lactose were purchased from R&M Chemicals Sdn. Bhd., Malaysia. All chemicals were used as received without purification.

2.2. Preparation of Mg-Al LDH

30 mmol magnesium nitrate hexahydrate [$Mg(NO_3)_2.6H_2O$] and 15 mmol aluminium nitrate nanohydrate [$Al(NO_3)_3.9H_2O$] were weighed separately in an analytical weighing balance. 50 ml of a solution containing 30 mmol magnesium nitrate hexahydrate and 15 mmol aluminum nitrate nanohydrate (Mg: Al = 2:1) were put together in a beaker.

2.3. Synthesis and exfoliation of Mg-Al LDH

Mg-Al LDH was prepared by following an established method (Co-precipitation) (15). The prepared Mg-Al LDH solution was added dropwise to 30 ml of distilled water mixed with 70 ml DMSO solution containing 1g of sucrose under stirring conditions. Throughout the mixing of the metal salt solutions, the pH of the reaction mixture was kept at 9 using 1 M of NaOH solution. The reaction was carried out under the nitrogen gas purge. The slurry product obtained was centrifuged for 3 minutes at 3500 rpm in 3 cycles. The resulting product was kept in a freezer dryer for 24 hours and the samples were mashed into a powder form for further characterization. The same procedure was repeated for 1g glucose and 1g lactose.

2.4. Characterizations

X-ray diffraction patterns of synthesized samples were recorded on a Bruker-D8 diffractometer using Cu-Kα radiation. The Fourier transform infrared spectra were recorded on an FTIR spectrometer (Perkin Elmer, System 2000) while the morphologies of LDH samples were analyzed using transmission electron microscopy (FEI Tecnai G2 F20). Thermal analysis of samples was recorded using the Perkin Elmer SDTA 6000 Thermogravimetric analyzer and differential scanning calorimetry measurements were obtained using the Perkin Elmer DSC instrument. The surface area was measured using a Brunauer Emmett-Teller instrument (Micromeritic ASAP 2020). A graph of the cumulative particle size distribution of exfoliated LDH was plotted to determine the median diameter of the particle.

3. RESULTS AND DISCUSSION

3.1. XRD

Figure 1 shows the typical X-ray diffraction (XRD) patterns of the synthesized LDH and its exfoliated diffraction patterns. Figure 1a shows the first basal reflection for pristine LDH at $2\theta = 10.3°$ corresponding to the basal spacing of $d_{003} = 8.6$ Å. (16). The d-spacing of pristine LDH calculated from the (003) peak was 8.6 Å, which well matched with that of previously reported NO_3^- intercalated LDH

(17). Other basal reflections are observed at 2θ = 20.2° corresponding to the basal spacing of d_{006} = 4.4 Å and 2θ = 29.6° corresponding to the basal spacing of d_{006} = 3.0 Å (16). Figure 1b shows the XRD pattern for LDH exfoliated with sucrose. The diffraction pattern exhibits a sharp peak at 2θ = 20.8°, corresponding to the basal spacing of d_{006} = 4.3 Å (17). The basal spacing of d_{006} is observed in Figure 1c (LDH exfoliated with glucose) and Figure 1d (LDH exfoliated with lactose). These basal spacings of d_{006} in all the exfoliated samples may indicate the formation of single-layer LDH nanosheets (18). For comparison, Figure 1e exhibits the stacked spectrum of LDH pristine and each LDH exfoliated with sucrose, glucose, and lactose, where the latter patterns indicate the formation of single-layer nanosheets. Figure 1f shows the XRD patterns for suspension samples (a)–(c). In all samples, single sharp peaks are observed at 2θ = 23.9°,22.4°, and 22.3° respectively, which correspond to the characteristic (006) basal reflection of LDH single layers (18). Figure 1g shows the XRD patterns for semi-dry samples (a)–(c). Similarly, sharp peaks are observed at 2θ = 20.4°, 21.4°, and 20.1° at the basal reflection (006) indicating the formation of single-layer LDH. The 2θ values for the semi-dry samples differ from the suspension samples due to the different hydration states and drying techniques (14). A broad peak is observed for suspension samples, maybe due to water molecules, whereas for semi-dry samples, the shape of the water peak is narrower (14).

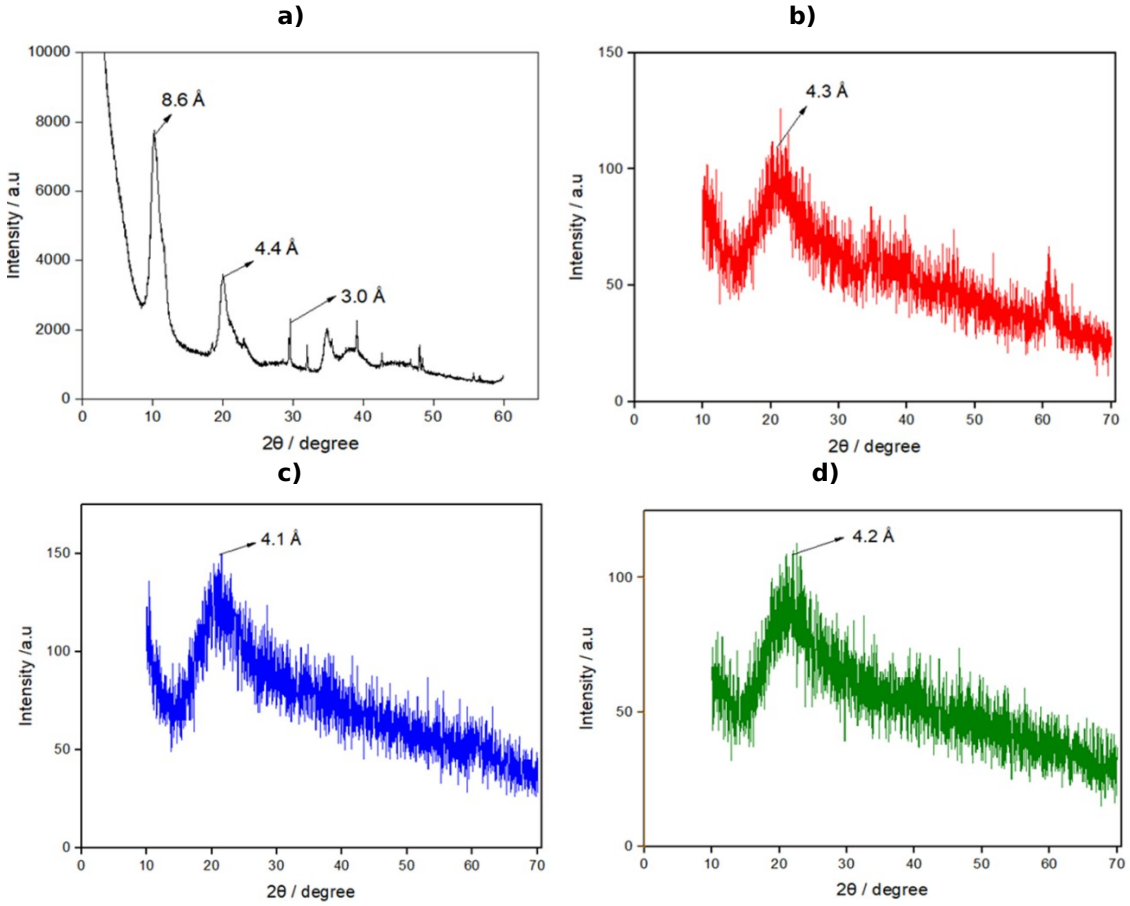

Figure 1: XRD pattern of a) LDH pristine b) LDH exfoliated with sucrose c) LDH exfoliated with glucose d) LDH exfoliated with lactose.

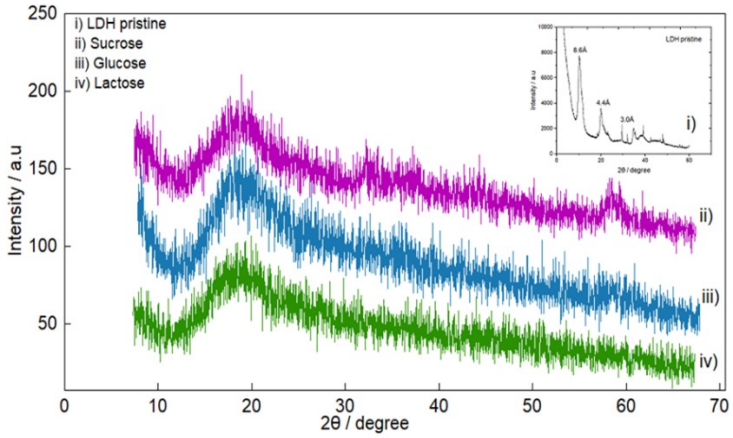

Figure 1e: Stacked XRD patterns of i) LDH pristine ii) LDH exfoliated with sucrose iii) LDH exfoliated with glucose iv) LDH exfoliated with lactose.

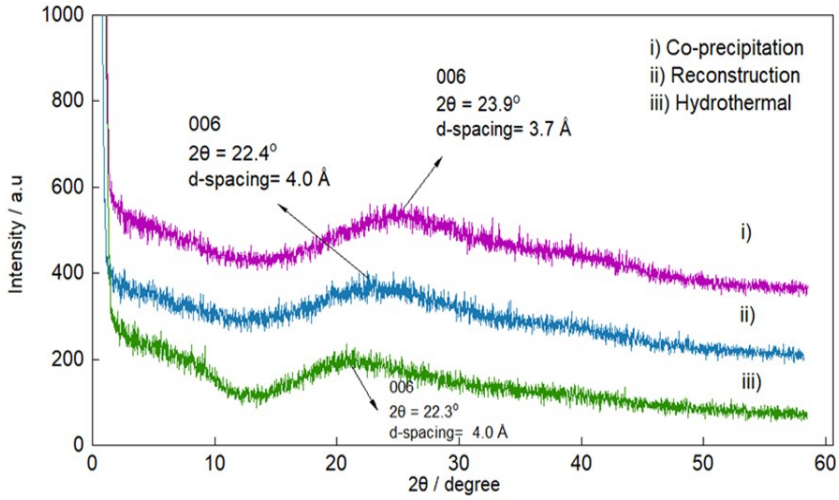

Figure 1f: X-ray diffraction pattern of suspension samples i) LDH exfoliated with sucrose (co-precipitation) ii) LDH exfoliated with sucrose (Reconstruction) iii) LDH exfoliated with sucrose (hydrothermal).

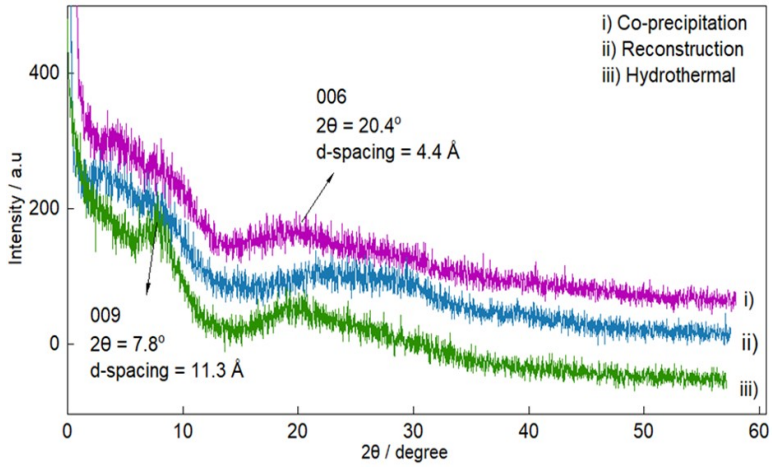

Figure 1g: X-ray diffraction pattern of semi-dry samples i) LDH exfoliated with sucrose (co-precipitation) ii) LDH exfoliated with sucrose (Reconstruction) iii) LDH exfoliated with sucrose (hydrothermal).

3.2. TGA

Figure 2 shows a thermogravimetric analysis of LDH pristine and LDH exfoliated with sucrose, glucose, and lactose. Figure 2a exhibits four decomposition stages of mass loss for the LDH pristine sample. The first mass loss of 10.9% at 210 ℃ was due to the loss of physically absorbed water (19). The second mass loss of 8.1% at 365 ℃ was due to water loss in the LDH interlayer regions. The third mass loss of 9.9% at 521 ℃ was attributed to the decompositions of carbonate and the hydroxyl layers in between the LDH layers. The final mass loss of 16.1% at 690℃ is due to the decomposition of the organic compound (19). A similar pattern is observed in LDH exfoliated with sucrose (Figure 2b). Three thermal steps occurred at 42.6, 247, and 404 ℃, registering the corresponding mass losses of 34.0, 24.7, and 5.3% respectively. The first mass loss is attributed to the loss of surface and interlayer water, whereas the second step might be due to the dehydroxylation of brucite sheets. The final step can be assigned to the decomposition of nitrate ions (20). Similarly, Figure 2c shows three thermal steps of mass losses which occurred at 39.6, 250.6, and 336.1 ℃, registering the corresponding mass losses of 53.1, 10.3, and 9.8% respectively. The first mass loss is due to the loss of surface and interlayer water, while the second step is attributed to the dehydroxylation of the brucite sheets. The final mass loss is due to the decomposition of organic compounds or the rest residues of LDH (21). The mass loss pattern is also observed in Figure 2d. The first mass loss of 45.5% at 103.5 ℃ was due to the removal of weekly adsorbed water, followed by the second one at 268 ℃ (correspondingly 15.6%); this is ascribed to dehydroxylation of the LDH lattices. The third mass loss of 3.1% at 460 ℃ is due to the decomposition of nitrate ions (20). Figure 2e shows the stacked spectrum of the TGA/DTG graph of LDH pristine, LDH exfoliated with sucrose, glucose, and lactose for comparison. The first mass loss percentage for LDH pristine is less compared to exfoliated samples. This might be due to more water loss during the exfoliation process. In conclusion, the TGA data have significantly enhanced the thermal stability of exfoliated LDH compared to LDH pristine.

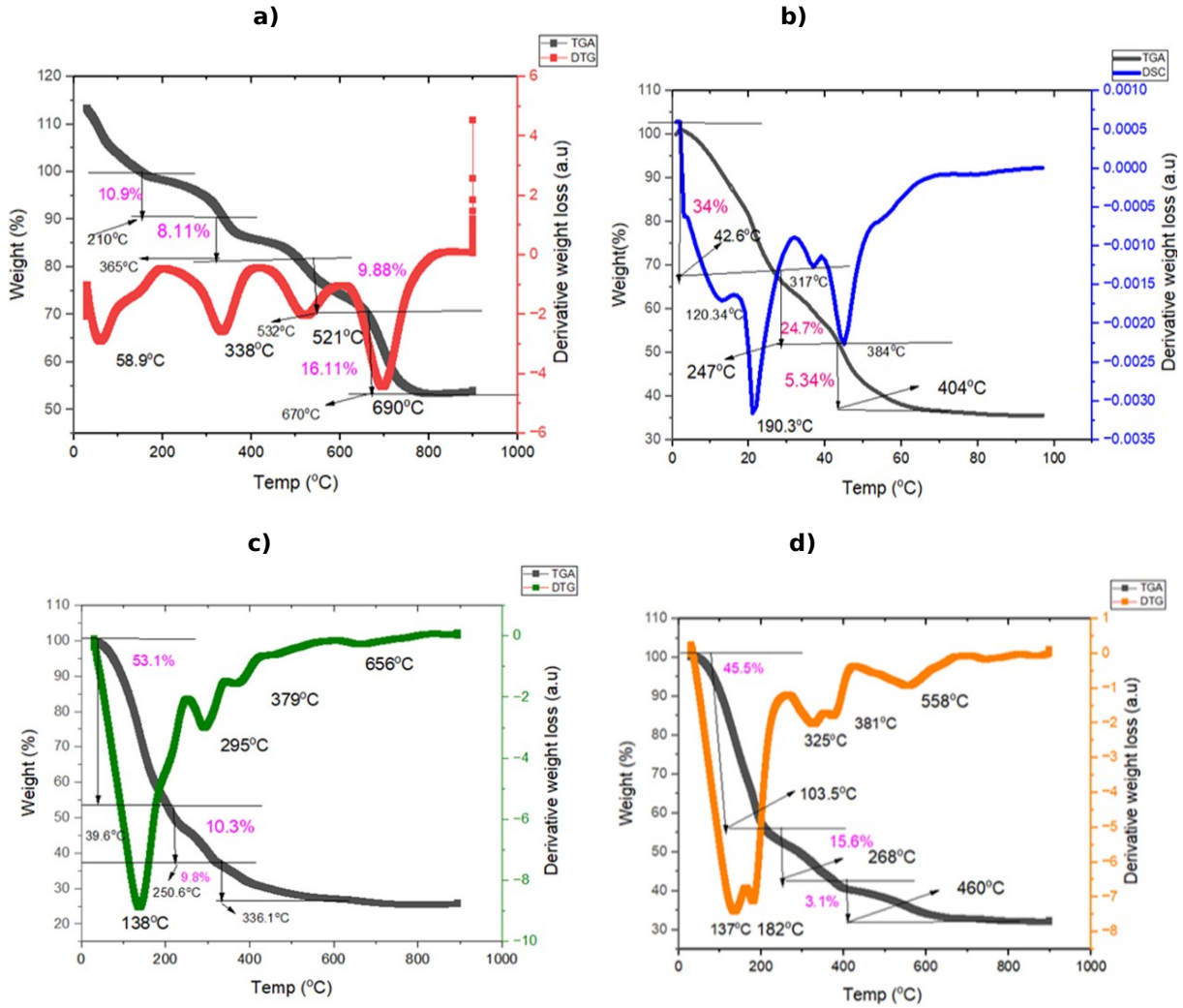

Figure 2: TGA/DTG graph of a) LDH pristine b) LDH exfoliated with sucrose c) LDH exfoliated with glucose c) LDH exfoliated with lactose.

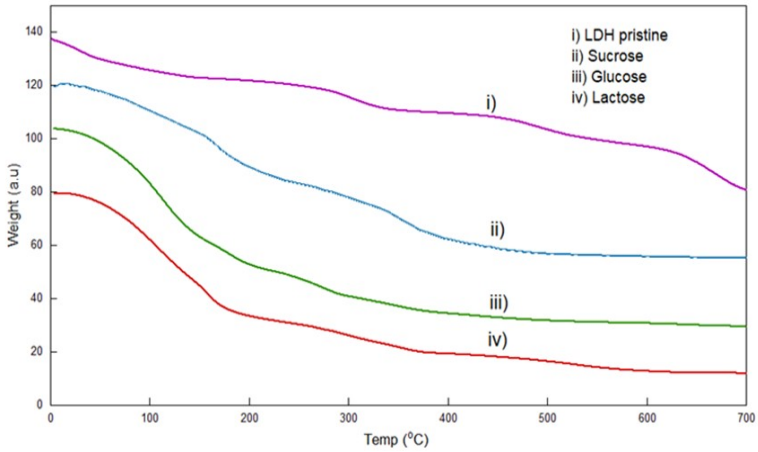

Figure 2e: Stack spectrum of TGA/DTG graph of i) LDH pristine ii) LDH exfoliated with sucrose iii) LDH exfoliated with glucose iv) LDH exfoliated with lactose.

3.3. DSC

Figure 3 shows differential scanning calorimetry (DSC) of LDH pristine and exfoliated LDH with sucrose, glucose, and lactose. Figure 3a exhibits three peaks at temperatures 276, 308, and 341 ℃. These peaks are due to the endothermic reaction caused by the melting process (22). The sharp endothermic peak at 308 ℃ might be due to an initial LDH de-hydroxylation of the metal hydroxide layers (23). Figure 3b shows two peaks at 113 and 380 ℃. These peaks are due to the endothermic reaction caused by the loss of adsorbed surface water (22). Figure 3c exhibits two peaks at 137 and 316 ℃. The peak at 137 ℃ was due to an endothermic reaction caused by melting, while the peak at 316 ℃ was due to an exothermic reaction caused by crystallization (22). In contrast, Figure 3d exhibits one sharp peak at 139 ℃ due to an endothermic reaction caused by melting. Figure 3e compares the stacked spectrum of DSC spectra of LDH pristine and exfoliated LDH with sucrose, glucose, and lactose. Exfoliated LDH samples show lower endothermic temperatures compared to LDH pristine. This might be due to more surface and interlayer water loss during the formation of LDH nanosheets. The DSC data have significantly enhanced the thermal stability of exfoliated LDH compared to LDH pristine.

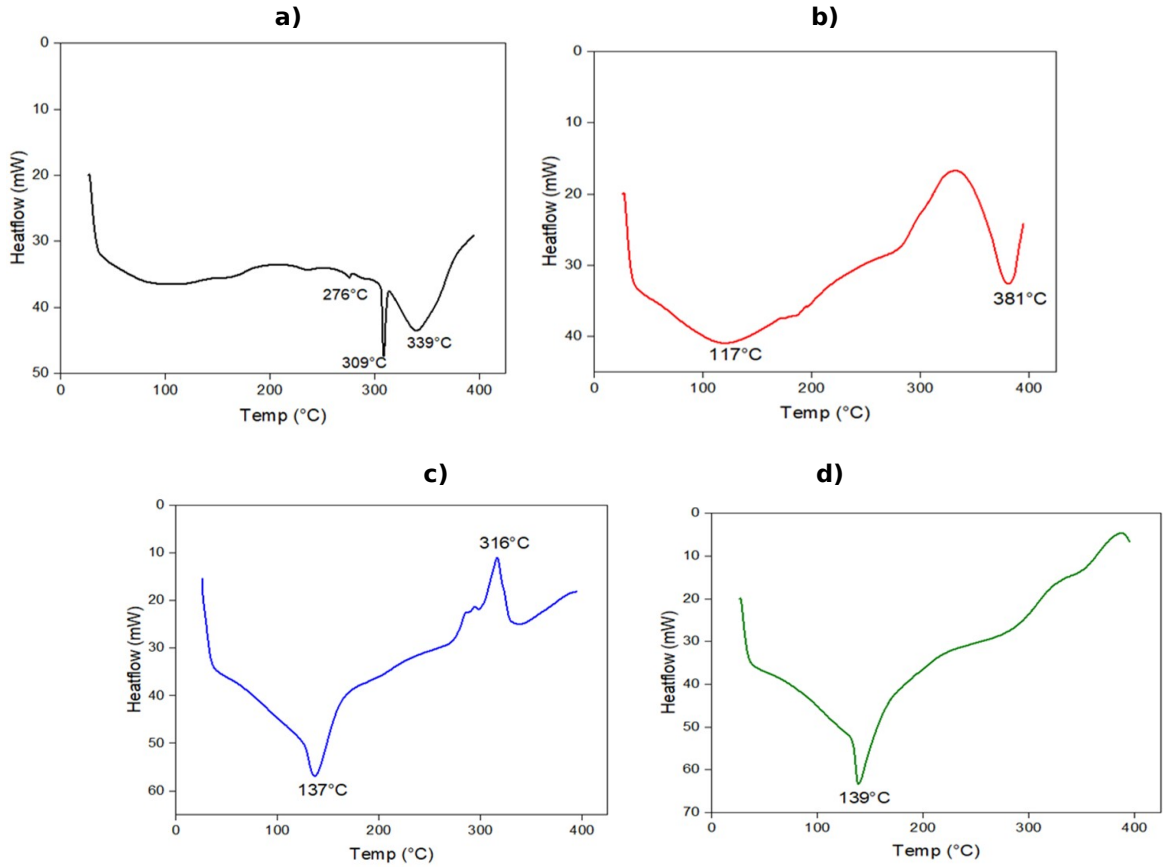

Figure 3: DSC graph of a) LDH pristine b) LDH exfoliated with sucrose c) LDH exfoliated with glucose d) LDH exfoliated with lactose.

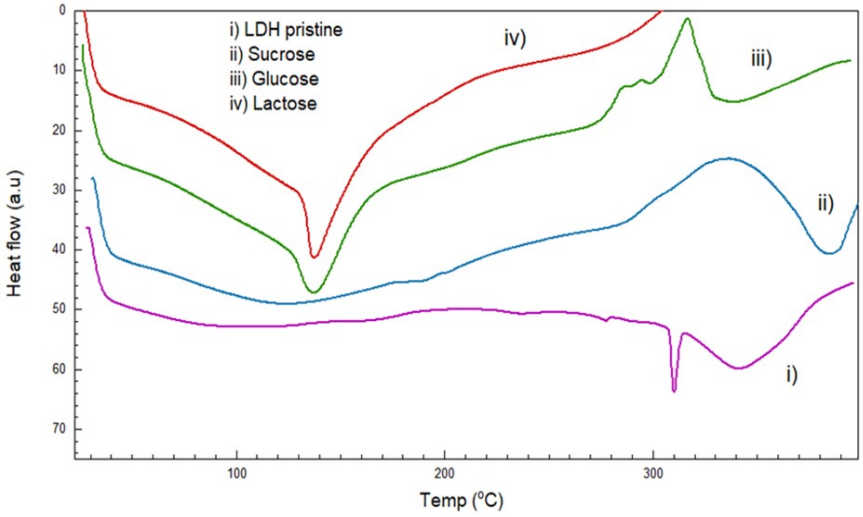

Figure 3e: Stack DSC graph of i) LDH pristine ii) LDH exfoliated with sucrose iii) LDH exfoliated with glucose iv) LDH exfoliated with lactose.

3.4. FTIR

Figures 4a, 4b, 4c, and 4d depict the FTIR spectra spectrum of LDH pristine and LDH exfoliated with glucose, lactose, and sucrose. Figures 4a, 4b, 4c, and 4d show absorption peaks in region 3400 cm^{-1}. These peaks were due to the O-H stretching of water molecules and hydroxyl groups in the lamellar structure (24). Figures 4a, 4b, 4c, and 4d also show absorption peaks at 1349, 1344, 1338, and 1390 cm^{-1}, respectively which are attributed to the vibration of carbonate species. The bands in the region of 900-1000 cm^{-1} were ascribed to the stretching of Al-O and Mg-O bonds (25). The band that occurred around 1600 cm^{-1} was attributed to O-H of interlayer water molecules, while the absorption band of nitrate ions was observed at 1390 cm^{-1}. The absorption peaks at the region 1000-1020 cm^{-1} in LDH pristine and exfoliated samples were due to C-H stretching (12). However, the intensity peak at the region 1000-1020 cm^{-1} for LDH exfoliated with sugar molecules is higher compared to LDH pristine due to the C-H stretching in sugar molecules which indicates the successful exfoliation of sugar molecules in the interlayer of LDH. All the bands that appeared in LDH pristine also appeared in exfoliated LDHs. This may indicate that LDH was successfully exfoliated into single-layer structures. Figure 4e demonstrates the stacked spectrum of LDH pristine and exfoliated LDH, where it shows the important bands of LDH. The bands present in LDH pristine in the region of 3400, 1600, and 1300 cm^{-1} are also present in exfoliated LDHs.

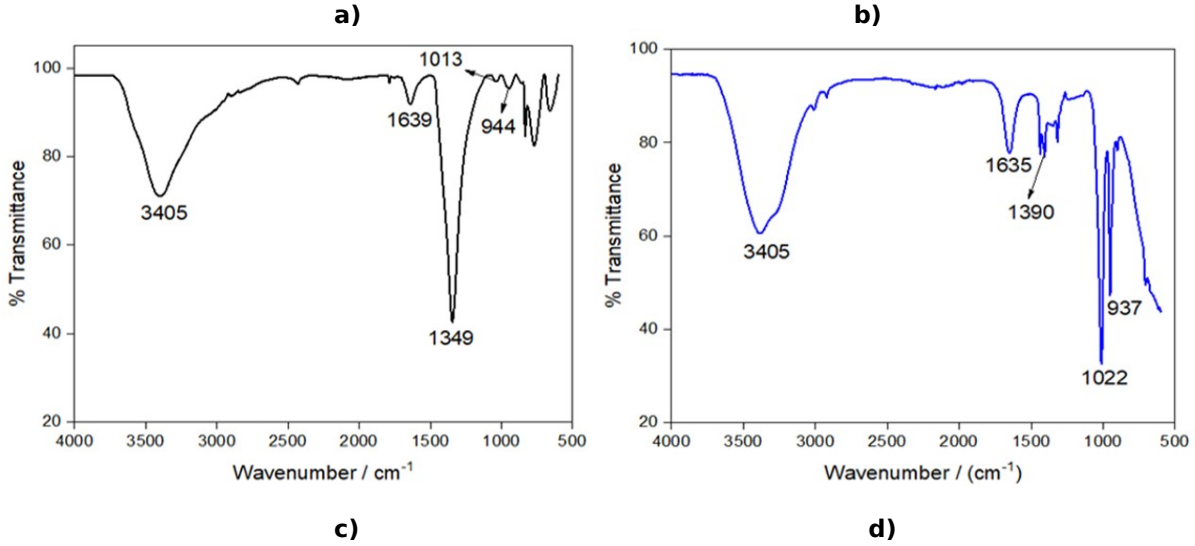

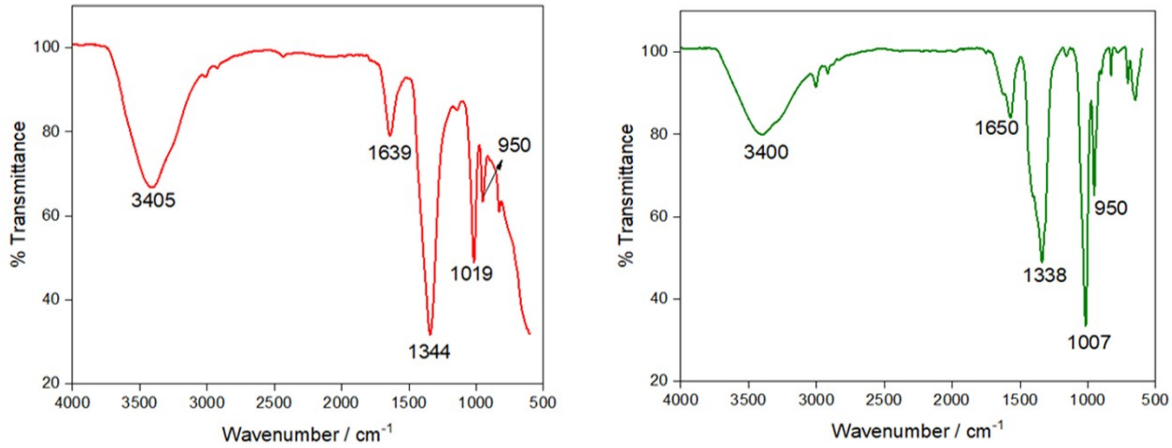

Figure 4: FTIR spectra of a) LDH pristine b) LDH exfoliated with sucrose c) LDH exfoliated with glucose c) LDH exfoliated with lactose.

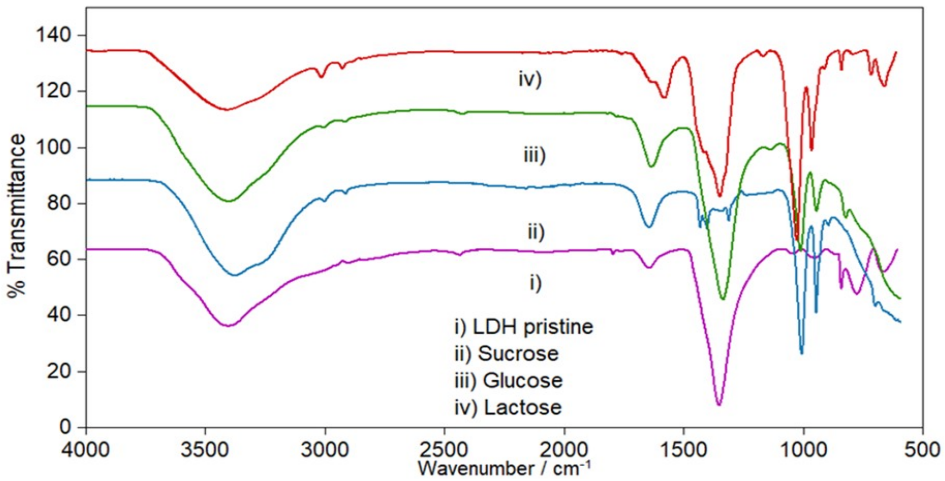

Figure 4e: Stacked FTIR spectra of i) LDH pristine ii) Exfoliated LDH with sucrose iii) Exfoliated LDH with glucose iv) Exfoliated LDH with lactose

3.5. Stack FTIR of suspension exfoliated LDH with sucrose by co-precipitation, hydrothermal, and reconstruction.

Figure 4f depicts the FTIR spectrum of suspension LDH exfoliated with sucrose. Three different preparation methods were employed for the suspension samples below, namely co-precipitation, reconstruction, and hydrothermal. All the suspension samples show absorption peaks in the region of 3400 cm^{-1}. These peaks were due to the O-H stretching of water molecules and hydroxyl groups in the lamellar structure (24). Besides, absorption peaks in the region of 1600 cm^{-1} are assigned to the stretching of the O-H of interlayer water molecules. The bands in the 900-1000 cm^{-1} region were ascribed to the stretching of Al-O and Mg-O bonds (24).

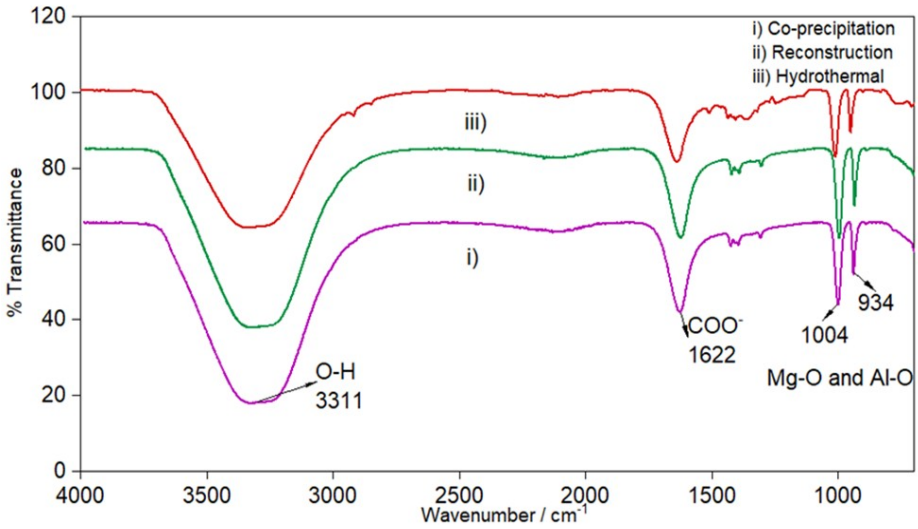

Figure 4f: Stacked FTIR spectra of suspension samples i) LDH exfoliated with sucrose (co-precipitation) ii) LDH exfoliated with sucrose (reconstruction) iii) LDH exfoliated with sucrose (hydrothermal).

3.6. Stack FTIR of semi-dry exfoliated LDH with sucrose by co-precipitation, hydrothermal, and reconstruction

Figure 4g shows FTIR spectroscopy analysis of semi-dry exfoliated LDH with sucrose. Different methods have been used for the semi-dry samples below such as co-precipitation, reconstruction, and hydrothermal. All the suspension samples show absorption peaks in the region 3400 cm^{-1}. These peaks are due to the O-H stretching of water molecules and hydroxyl groups in the lamellar structure (25). Besides, absorption peaks at the region 1600 cm^{-1} due to O-H of interlayer water molecules. The bands in the 900-1000 cm^{-1} region are ascribed to the stretching of Al-O and Mg-O bonds (24). Absorption peaks at the region 1300 cm^{-1} due to the vibration of nitrate ions. FTIR makes it easy to determine the functional groups and possible interactions between intercalated anions and inorganic lamellae.

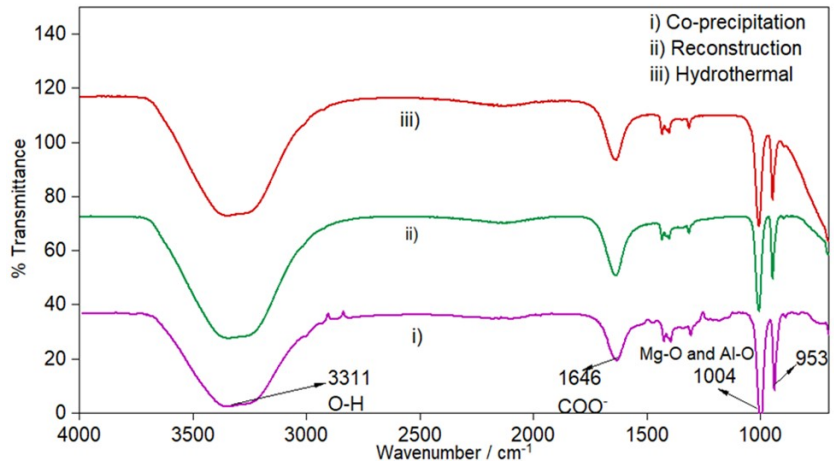

Figure 4g: Stacked FTIR spectra of semi-dry samples i) LDH exfoliated with sucrose (co-precipitation) ii) LDH exfoliated with sucrose (reconstruction) iii) LDH exfoliated with sucrose (hydrothermal).

3.7. BET

Figure 5 shows the nitrogen adsorption-desorption isotherms of LDH pristine and LDH exfoliated with sucrose, glucose, and lactose. Figure 5a shows the LDH pristine, where it displays type IV sorption isotherms with a H3 hysteresis loop. This loop belongs to mesoporous materials, composed of plate-like substances with agglomerating slit-shaped pores (26). Figures 5b, 5c, and 5d show LDH exfoliated with sucrose, glucose, and lactose. They display H2-type loops where the distributions of pore size radius are wide (27). Compared to LDH pristine, LDH exfoliated with sucrose, glucose, and lactose shows a broad adsorption branch. This is due to the increase in basal spacing during the exchange of sugar molecules into the interlayer LDH (27). The adsorption and desorption curves of sucrose do not overlap in low relative pressure, indicating that sucrose molecules form strong chemical bonds with the adsorption sites, resulting

in a slow desorption rate and incomplete desorption (29). The wide hysteresis loop for the exfoliated LDHs proved the successful exfoliation of sugar molecules into LDH layers.

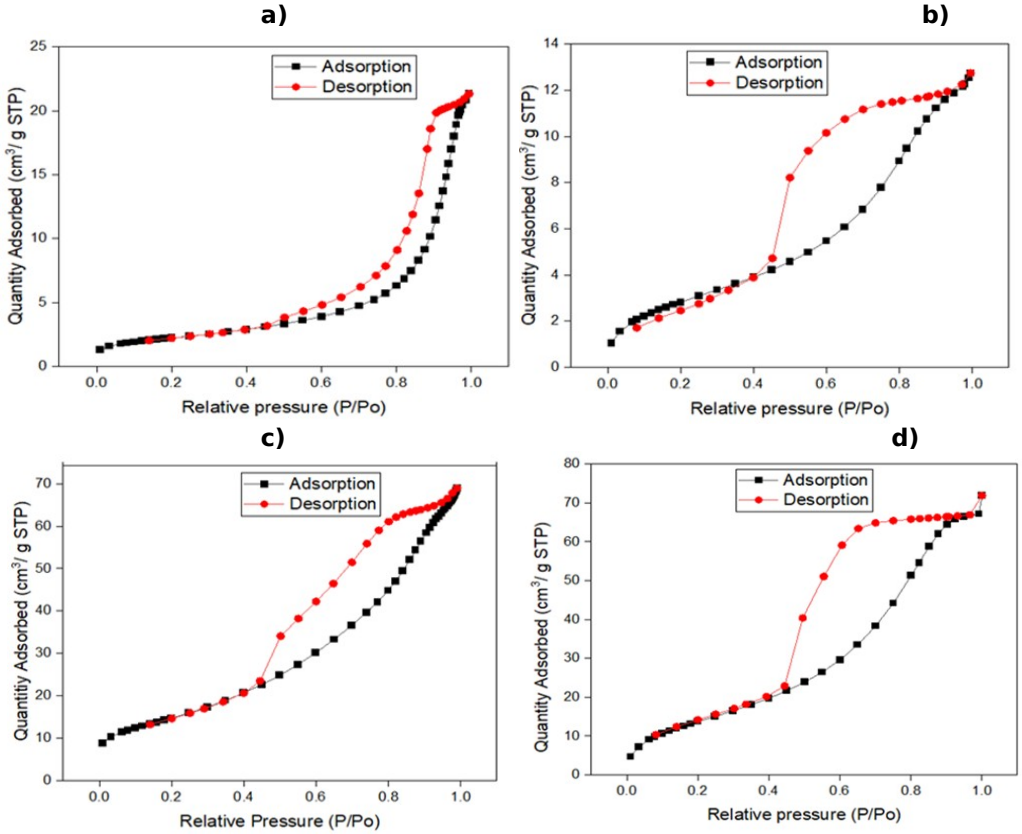

Figure 5: BET graph of a) LDH pristine b) LDH exfoliated with sucrose c) LDH exfoliated with glucose d) LDH exfoliated with lactose.

3.8. TEM

The formation of the LDH nanosheet was observed using transmission electron microscopy (TEM). Figure 6a reveals that LDH exfoliated with sucrose (co-precipitation suspension) has dark, agglomerated spherical-like particles (30). LDH nanosheets can be observed in Figure 6b (co-precipitation semi-dry) and in Figure 6c (co-precipitation fully dried) with a thickness of 4.35 nm and 3.98 nm respectively (31). Figure 6d shows agglomerated dark particles for LDH exfoliated with sucrose (reconstruction suspension). Both Figure 6e (reconstruction semi-dry) and 6f (reconstruction fully dried) show spherical-like particles. TEM image of exfoliated LDH nanosheets can be observed with a thickness of 2.68 nm in Figure 6g (hydrothermal suspension). LDH exfoliated with sucrose (hydrothermal semi-dry) reveals a dark spherical-like particle with a diameter of 8.15 nm in Figure 6h while LDH exfoliated with sucrose (hydrothermal fully dried) reveals a spherical-like particle with a diameter of 3.01 nm in Figure 6i.

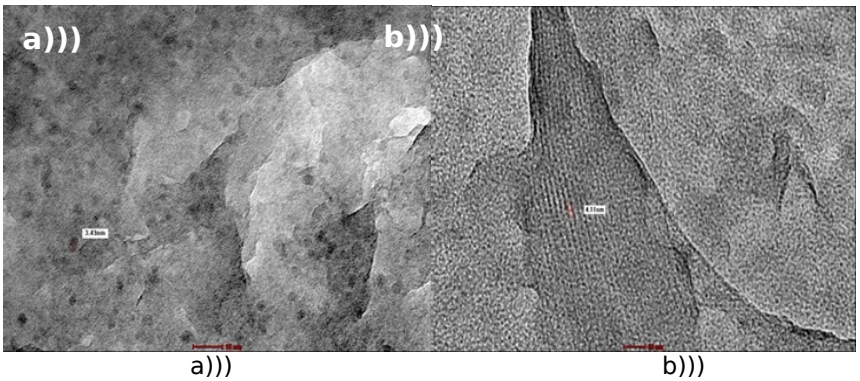

a))) b)))

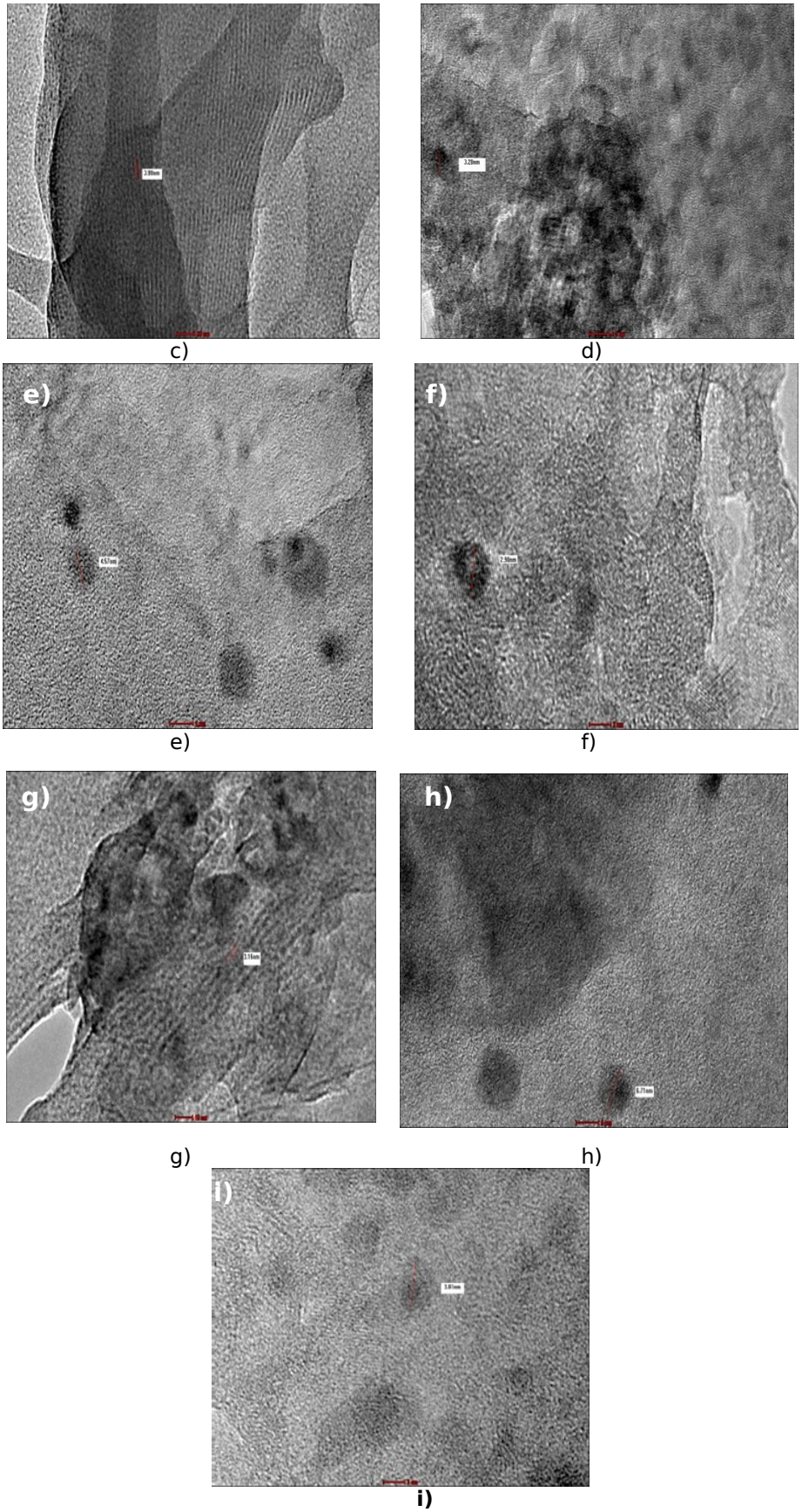

Figure 6: TEM images of exfoliated LDH with sucrose a) Co-precipitation suspension b) Co-precipitation semi-dried c) Co-precipitation fully dried d) Reconstruction suspension e) Reconstruction semi-dried f) Reconstruction fully dried g) Hydrothermal suspension h) Hydrothermal semi-dried i) Hydrothermal fully dried.

4. CONCLUSION

The exfoliation of LDH has emerged as a highly promising and rapidly advancing research area, primarily due to its extensive applications and potential in the field of material sciences. Sugar molecules have demonstrated their potential as an effective exfoliating agent for the exfoliation of layered double hydroxides (LDH) without the need for pre-intercalation of the layered material. The exfoliation of LDH has been successfully confirmed through a comprehensive analysis using various techniques including X-ray diffraction (XRD), Fourier transform infrared spectroscopy (FTIR), transmission electron microscopy (TEM), thermogravimetric analysis (TGA), differential scanning calorimetry analysis (DSC), and Brunauer-Emmett-Teller (BET) analysis. These techniques collectively provide strong evidence for the exfoliation of LDH. The presence of a singular peak in the X-ray diffraction (XRD) analysis indicates that the exfoliation process effectively produced individual layers of LDH nanosheets. Besides, a study is conducted on the crystalline state of layered double hydroxide (LDH) at various phases during the process of liquid exfoliation. This investigation encompassed the stages of suspension, semi-dry suspension, and dried solid samples. The X-ray diffraction (XRD) study indicates the presence of a distinct and prominent peak, suggesting the successful development of single-layer nanosheets. Fourier transform Infrared (FTIR) analysis also provides evidence of the effective exfoliation of multilayer materials. All the bands observed in LDH pristine samples were likewise observed in exfoliated LDHs and the intensity of the peaks for the exfoliated LDH is higher compared to pristine LDH. In addition, the thermal stability of LDH exfoliated samples is greatly enhanced through the utilization of TGA and DSC analysis. The mass loss percentage of exfoliated double hydroxide (LDH) is greater than pristine LDH. The broad hysteresis loops seen in the BET analysis of exfoliated LDHs provide evidence of the successful incorporation of sugar molecules into the LDH layers. The application of transmission electron microscopy (TEM) yielded significant findings about the formation of LDH nanosheets and pseudohexagonal particles in exfoliated LDHs. In summary, there is a pressing need for the development of environmentally friendly techniques for the exfoliation of layered double hydroxides (LDHs).

5. CONFLICT OF INTEREST

The authors declare no conflict of interest.

6. ACKNOWLEDGMENTS

This research was supported by the Ministry of Higher Education Malaysia under the Fundamental Research Grant Scheme (FRGS) with Grant no: 203/PKIMIA/6711925.

7. REFERENCES

1. Ghazali SA, Fatimah I, Bohari FL. Synthesis of Hybrid Organic-Inorganic Hydrotalcite-Like
Materials Intercalated with Duplex Herbicides: The Characterization and Simultaneous Release
Properties. Vol. 26, Molecules. 2021.

2. Gorrasi G, Sorrentino A. Layered double hydroxide polymer nanocomposites for food-packaging applications. Layer Double Hydroxide Polym Nanocomposites. 2020;743–79.

3. Zhang Y, Xu H, Lu S. Preparation and application of layered double hydroxide nanosheets. RSC Adv [Internet]. 2021;11(39):24254–81. Available from: <URL>.

4. Munonde TS, Zheng H, Nomngongo PN. Ultrasonic exfoliation of NiFe LDH/C nanosheets for enhanced oxygen evolution catalysis. Ultrason Sonochem. 2019;59:104716.

5. Karthikeyan J, Fjellvåg H, Bundli S, Sjåstad AO. Efficient Exfoliation of Layered Double Hydroxides; Effect of Cationic Ratio, Hydration State, Anions and Their Orientations. Materials (Basel) [Internet]. 2021 Jan 2 [cited 2022 Oct 12];14(2):1–11.

6. Joshi D, Adhikari N. An Overview on Common Organic Solvents and Their Toxicity. J Pharm Res Int. 2019 Jun 29;1–18.

7. Chen Z, Fan Q, Huang M, Cölfen H. Synthesis of two-dimensional layered double hydroxides: a systematic overview. CrystEngComm [Internet]. 2022;24(26):4639–55. Available from: <URL>.

8. Niu Y, Zheng C, Xie Y, Kang K, Song H, Bai S, et al. Efficient Adsorption of Ammonia by Surface-Modified Activated Carbon Fiber Mesh. Vol. 13, Nanomaterials. 2023.

9. Verheijen M, Lienhard M, Schrooders Y, Clayton O, Nudischer R, Boerno S, et al. DMSO induces drastic changes in human cellular processes and epigenetic landscape in vitro. Sci Reports 2019 91 [Internet]. 2019;9(1):1–12. Available from: <URL>.

10. Zhitova E, Krivovichev S, Yakovenchuk V, Ivanyuk G, Pakhomovsky Y, Mikhailova J. Crystal chemistry of natural layered double hydroxides. 4. Crystal structures and evolution of structural complexity of quintinite polytypes from the Kovdor alkaline massif, Kola peninsula, Russia. Mineral Mag. 2017 Jul 11;82.

11. Chen K, Zhang W, Pan X, Huang L, Wang J, Yang Q, et al. Natural Sugar: A Green Assistance to Efficiently Exfoliate Inorganic Layered Nanomaterials. Inorg Chem. 2018 May 7 ;57(9):5560–6. Available from: <URL>.

12. Chen S, Xu R, Liu J, Zou X, Qiu L, Kang F, et al. Simultaneous Production and Functionalization of Boron Nitride Nanosheets by Sugar-Assisted Mechanochemical Exfoliation. AdvMater.2019 Mar 1;31(10):1804810. Available from: <URL>.

13. Hoenig E, Strong SE, Wang M, Radhakrishnan JM, Zaluzec NJ, Skinner JL, et al. Controlling the Structure of MoS2 Membranes via Covalent Functionalization with Molecular Spacers. Nano Lett [Internet]. 2020 Nov 11;20(11):7844–51. Available from: <URL>.

14. Bae HJ, Goh Y, Yim H, Yoo SY, Choi J-W, Kwon D-K. Atomically thin, large area aluminosilicate nanosheets

fabricated from layered clay minerals. Mater Chem Phys [Internet]. 2019;221:168–77. Available from: <URL>.

15. Matusik J, Hyla J, Maziarz P, Rybka K, Leiviskä T. Performance of Halloysite-Mg/Al LDH Materials for Aqueous As(V) and Cr(VI) Removal. Materials (Basel) [Internet]. 2019;12(21).

16. Naik B, Arulraj J, Kolinjavadi M, Rajamathi M. Solvent-Mediated and Mechanochemical Methods for Anion Exchange of Carbonate from Layered Double Hydroxides Using Ammonium Salts. ACS Omega. 2019 Nov 12;XXXX.

17. Liang J, Ma R, Iyi N, Ebina Y, Takada K, Sasaki T. Topochemical Synthesis, Anion Exchange, and Exfoliation of Co−Ni Layered Double Hydroxides: A Route to Positively Charged Co−Ni Hydroxide Nanosheets with Tunable Composition. Chem Mater. 2010 Jan 26;22(2):371–8. Available from: <URL>.

18. Kansal S, Singh P, Biswas S, Chowdhury A, Mandal D, Priya S, et al. Superior-catalytic performance of Ni–Co layered double hydroxide nanosheets for the reduction of p-nitrophenol. Int J Hydrogen Energy [Internet]. 2023;48(56):21372–82. Available from: <URL>

19. Magri VR, Duarte A, Perotti GF, Constantino VRL. Investigation of Thermal Behavior of Layered Double Hydroxides Intercalated with Carboxymethylcellulose Aiming Bio-Carbon Based Nanocomposites. Vol. 3, ChemEngineering. 2019.

20. Ebadi M, Buskaran K, Saifullah B, Fakurazi S, Hussein MZ. The Impact of Magnesium–Aluminum-Layered Double Hydroxide-Based Polyvinyl Alcohol Coated on Magnetite on the Preparation of Core-Shell Nanoparticles as a Drug Delivery Agent. Int J Mol Sci [Internet]. 2019;20(15). Available from: <URL>.

21. Rosa-Guzmán M, Guzman A, Cayetano-Castro N, Del Rio J, Corea M, Martínez-Ortiz M. Thermal Stability Evaluation of Polystyrene-Mg/Zn/Al LDH Nanocomposites. Nanomaterials. 2019 Oct 27;9:1528.

22. Ghanbari E, Picken SJ, van Esch JH. Analysis of differential scanning calorimetry (DSC): determining the transition temperatures, and enthalpy and heat capacity changes in multicomponent systems by analytical model fitting. J Therm Anal Calorim [Internet]. 2023;148(22):12393–409. Available from: <URL>.

23. Zhitova ES, Greenwell HC, Krzhizhanovskaya MG, Apperley DC, Pekov I V, Yakovenchuk VN. Thermal Evolution of Natural Layered Double Hydroxides: Insight from Quintinite, Hydrotalcite, Stichtite, and Iowaite as Reference Samples for CO3- and Cl-Members of the Hydrotalcite Supergroup. Vol. 10, Minerals. 2020.

24. Hashim N, Sharif SNM, Isa IM, Ali NM, Damanhuri MIM. Synthesis and Characterisation of Zinc/Aluminium-Layered Double Hydroxide-L-Phenylalanate Nanocomposites Using Ion Exchange Method. Educ J Sci Math Technol. 2017 Jun 15 ;4(1):24–33. Available from: <URL>.

25. Razak NIA, Yusoff NISM, Wahit MU. Characterization and Thermal Behaviour of Magnesium-Aluminium Layered Double Hydroxide. J Adv Res Exp Fluid Mech Heat Transf. 2021 Dec 23;5(1):1–9. Available from:<URL>.

26. Szymaszek-Wawryca A, Díaz U, Samojeden B, Motak M. Synthesis, Characterization, and NH3-SCR Catalytic Performance of Fe-Modified MCM-36 Intercalated with Various Pillars. Vol. 28, Molecules. 2023.

27. Zhang L-Y, Han Y-L, Liu M, Deng S-L. Ni–Al layered double hydroxide-coupled layered mesoporous titanium dioxide (Ni–Al LDH/LM-TiO2) composites with integrated adsorption-photocatalysis performance. RSC Adv [Internet]. 2023;13(25):16797–814. Available from: <URL>.

28. Bohari F, Noor N, Sheikh mohd ghazali S ahmad izaddin, Dzulkifli N, Fatimah I, Adam N. Synthesis and Characterization of 2,4-Dichlorophenoxypropanoic Acid (2,4-DP) Herbicide Interleaved into Calcium-Aluminium Layered Double Hydroxide and the Study of Controlled Release Formulation. Indones J Chem. 2022 Aug 9;22:1330.

29. Niu Y, Zheng C, Xie Y, Kang K, Song H, Bai S, et al. Efficient Adsorption of Ammonia by Surface-Modified Activated Carbon Fiber Mesh. Vol. 13, Nanomaterials. 2023.

30. Nagendra B, Rosely CVS, Leuteritz A, Reuter U, Gowd EB. Polypropylene/Layered Double Hydroxide Nanocomposites: Influence of LDH Intralayer Metal Constituents on the Properties of Polypropylene. ACS Omega. 2017 Jan 31;2(1):20–31.
Available from: <URL>.

31. Abinaya R, Archana J, Harish S, Navaneethan M, Ponnusamy S, Muthamizhchelvan C, et al. Ultrathin layered MoS2 nanosheets with rich active sites for enhanced visible light photocatalytic activity. RSC Adv. 2018;8(47):26664–75. Available from: <URL> .